

# Lithium-loaded scintillators coupled to a custom-designed silicon photomultiplier array for neutron and gamma-ray detection

Felix Liang, *Member, IEEE*, Hartmut Brands, *Member, IEEE*, Les Hoy, *Member, IEEE*,  
Jeff Preston, *Member, IEEE*, and Jason Smith *Member, IEEE*,

**Abstract**—Scintillators capable of detecting both neutrons and gamma-rays have generated considerable interest. In particular, the use of such scintillators with silicon photomultipliers (SiPMs) enables low-power and compact-geometry applications. Three types of Li-loaded scintillators, CLYC, CLLB, and NaIL, have been tested with a custom-designed SiPM array for temperatures between  $-20$  and  $50^\circ\text{C}$ . The array consists of four  $6\times 6\text{ mm}^2$  SiPMs arranged in a  $2\times 2$  configuration. Pulse shape discrimination is used for neutron and gamma identification. Because the pulse shape changes with temperature, the quality of neutron and gamma discrimination varies with temperature. Furthermore, the larger dark current in SiPMs at high temperatures results in poorer energy resolution and neutron-gamma discrimination. Comparison of the energy resolution and the neutron-gamma discrimination for the three scintillators coupled to the custom SiPM array will be discussed.

## I. INTRODUCTION

Helium-3 filled neutron detectors have been widely used in basic science research, industrial applications, and homeland security. Since the recent  $^3\text{He}$  shortage, a great deal of effort has been dedicated to find replacement materials for neutron detection [1]. Some Li-loaded scintillators that are capable of detecting both neutrons and gamma-rays have generated considerable interest. When enriched  $^6\text{Li}$  is used in these scintillators, the sensitivity for neutron detection can be comparable to or exceed  $^3\text{He}$  tubes.

The recent advance in silicon photomultipliers (SiPMs) has made the photo detection efficiency similar to the conventional photomultiplier tubes (PMTs). Due to the compact size, ruggedness, low operating voltage, and insensitivity to magnetic fields, SiPMs have replaced PMTs as the photo sensor in some scintillation detectors. However, the active area of the largest SiPMs is far smaller than that of PMTs. Since the sensitivity of a radiation detector increases with the detector size, it is necessary to assemble SiPMs in an array for larger scintillators. A  $2\times 2$  SiPM array has been designed and constructed for coupling with 18 mm cubic scintillators [5]. The gain of the SiPMs in the array are matched in the temperature range between  $-20$  and  $50^\circ\text{C}$  for optimizing the energy resolution. With this SiPM array coupled to an 18 mm CsI cube, energy resolution of 6.4% for the 662 keV gamma-ray has been observed.

Felix Liang, Hartmut Brands, Les Hoy, and Jason Smith are with FLIR Systems Inc.

Jeff Preston, formerly with FLIR Systems Inc., is now with Consolidated Nuclear Security, LLC.

TABLE I

DENSITY ( $\rho$ ), WAVELENGTH OF MAXIMUM EMISSION ( $\lambda$ ), LIGHT YIELD (PH/MEV), AND DECAY TIME ( $\tau_d$ ) OF CLYC, CLLB, AND NaIL.

scintillator	CLYC	CLLB	NaIL
$\rho$ ( $\text{g/cm}^3$ )	3.3	4.2	3.6
$\lambda$ (nm)	370	420	418
ph/MeV	20,000	45,000	35,000
$\tau_d$	1, 50, 1000	180, 1140	230, 1000

This work investigates the performance of  $\text{Cs}_2\text{LiYCl}_6:\text{Ce}$  (CLYC) [2],  $\text{Cs}_2\text{LiLaBr}_6:\text{Ce}$  (CLLB) [3], and  $\text{NaI:Tl,Li}$  (NaIL) [4] coupled to the custom SiPM array for neutron and gamma-ray detection. Some physical properties of these scintillators are given in Table I.

## II. EXPERIMENTAL METHODS

Two CLYC scintillators that were manufactured in 2014<sup>1</sup> and 2016<sup>2</sup>, were used in this experiment. The CLYC and CLLB<sup>3</sup> scintillators were 18 mm cubes. One of the surfaces was coupled to the custom SiPM array where four  $6\times 6\text{ mm}^2$  SensL C-Series SiPMs were arranged in a  $2\times 2$  configuration. The rest of the scintillator surfaces were wrapped with PTFE tape. The scintillator and SiPM array were enclosed in a hermetically sealed aluminum can to keep out moisture. The detectors were packaged in a dry glove box in the laboratory.

The NaIL<sup>4</sup> scintillator was a 1.5-inch right cylinder encapsulated in an aluminum can. The scintillation light was transmitted out of one end of the cylinder by a quartz window and detected by the SiPM array. Because the 1.5-inch circular area is considerably larger than the footprint of the SiPM array, the exposed window area was covered with PTFE tape to reduce light loss.

The detector output was amplified by a Canberra 2022 spectroscopic amplifier and recorded by a CAEN V1785N peak-sensing ADC for studying the gamma-ray spectra. A Struck SIS3302 waveform digitizer was used to record the detector output for analyzing the pulse shape to discriminate neutrons from gamma-photons. Because there is a long-decay component of the pulses, the waveform digitizer stored each trace in a 10 ns interval for 5  $\mu\text{s}$ .

<sup>1</sup>Radiation Monitoring Devices, Inc.

<sup>2</sup>CapeSym Inc.

<sup>3</sup>Saint-Gobain

<sup>4</sup>Saint-Gobain

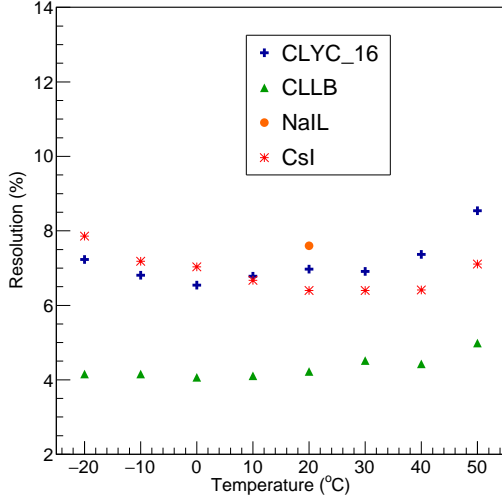


Fig. 1. Energy resolution for CLYC (crosses), NaIL (circles), and CLLB (triangles) as a function of temperature. CLYC\_16 is the CLYC scintillator manufactured in 2016. The energy resolution for CsI (asterisks) is shown for comparison.

### III. RESULTS AND DISCUSSION

#### A. Energy Resolution

The energy resolution of the detectors were measured with a  $^{137}\text{Cs}$  source for temperatures between  $-20$  and  $50^\circ\text{C}$ . Figure 1 shows the energy resolution as a function of temperature. The energy resolution for CLYC\_16 is 7.0% at  $20^\circ\text{C}$ . The variation of energy resolution with temperature is moderate and similar to the CsI detector of the same dimensions.

The energy resolution as a function of temperature was also measured for CLYC\_14. The procedures for assembling the detector were not the same as other detectors. The results are not presented in the figure because the comparison would not be fair. Moreover, CLYC is known to be fragile under temperature changes and this crystal might have developed fractures during the experiment. In spite of that, the ability to discriminate between neutron and gamma radiation is not affected as seen in the next section.

The energy resolution for the CLLB detector is 4.2% at  $20^\circ\text{C}$  and varies very little with temperature. For temperatures below  $20^\circ\text{C}$ , the energy resolution improved slightly. In contrast, the energy resolution gets worse for temperatures above  $30^\circ\text{C}$ . Degradation of energy resolution is observed for all the detectors studied in this work. This phenomenon is attributed to the higher dark current in the SiPMs at high temperatures.

The energy resolution for the NaIL detector is 7.6% at  $20^\circ\text{C}$ . In contrast, the energy resolution is 6.9% when the NaIL scintillator was coupled to a 3-inch PMT. The large mismatch of the contact area between the NaIL scintillator and the SiPM array results in worse energy resolution. For this reason, the energy resolution for NaIL was not measured at other temperatures.

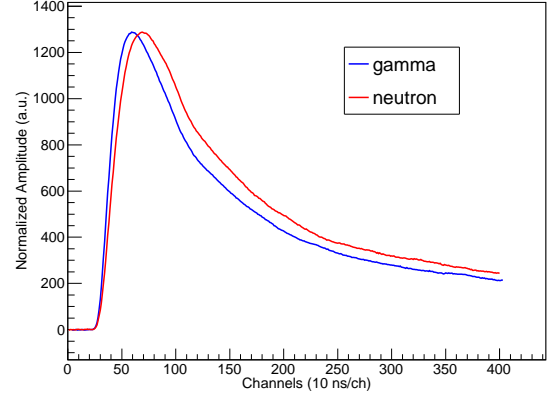


Fig. 2. Pulses for gamma (red curve) and neutron (blue curve) detected by CLYC at  $20^\circ\text{C}$ .

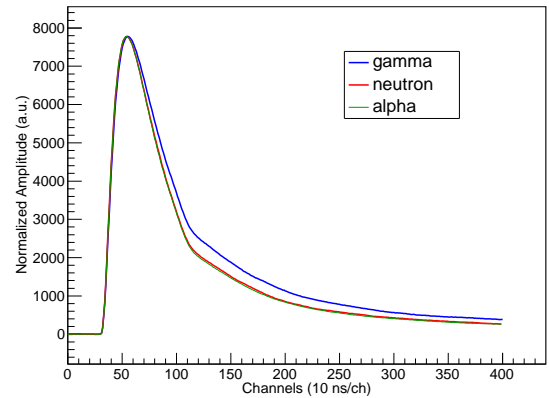


Fig. 3. Pulses for gamma (red curve), neutron (blue curve), and alpha (green curve) detected by CLLB at  $20^\circ\text{C}$ .

#### B. Pulse Shape Discrimination

Although the gamma-equivalent energy for neutrons is greater than 3 MeV for all three scintillators, CLYC, CLLB, and NaIL, these scintillators will also respond to high energy cosmic-rays. The fact that the pulse shape for neutrons is different from that of gammas and cosmic background allows the use of pulse shape discrimination (PSD) for neutron identification. While the difference in pulse shape between neutrons and gammas is in the rise time for CLYC, the difference in pulse shape is in the decay time for CLLB and NaIL. Figure 2, 3, and 4 displays the pulses for neutrons and gammas detected by CLYC, CLLB, and NaIL, respectively, at  $20^\circ\text{C}$ . These pulses, shown in the figures, are the average of 10 pulses for each type of radiation and the averaged gamma pulses are normalized to the maximum of the averaged neutron pulses.

In this work, the PSD is accomplished by taking the ratio of the time integral of the pulse with a short gate (Prompt) to that with a long gate (Prompt+Delay).

$$PSD = \frac{Prompt}{Prompt + Delay}, \quad (1)$$

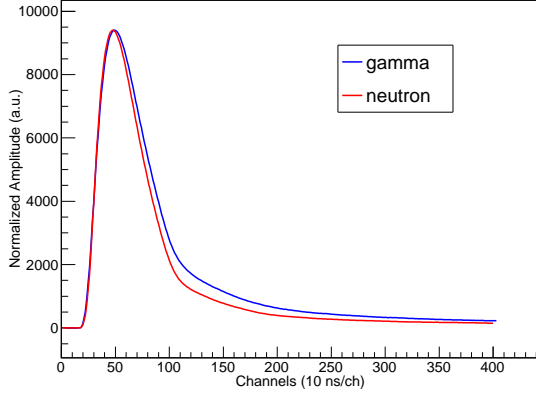


Fig. 4. Pulses for gamma (red curve) and neutron (blue curve) detected by NaIL at 20°C.

Figure 5(a) displays the scatter plot of the PSD ratio versus the integral of the long gate, which is equivalent to the gamma energy, for the measurement with NaIL at 20 °C. Neutron events can be seen as the isolated group above channel 3000. The events extending from channel 1000 to 3800 are from gammas. Two groups of gamma events between channel 1000 and 1500 are the 1.17 and 1.33 MeV gamma-rays from  $^{60}\text{Co}$ . Lower energy gamma events were ignored by setting the threshold of the constant fraction discriminator. Figure 5(b) shows the projection of events in the rectangular area in Fig. 5(a) onto the PSD ratio axis.

To quantify neutron and gamma discrimination, a figure of merit (FOM) is defined as

$$FOM = \frac{|\mu_\gamma - \mu_n|}{w_\gamma + w_n}, \quad (2)$$

where  $\mu$  and  $w$  are the centroid and full-width-at-half-maximum, respectively, of neutron and gamma distributions in the histogram of PSD ratio.

The pulse shape changes with temperature for all three detectors. Shown in Fig. 6 are the pulses for neutrons detected by NaIL at -20, 0, 20, and 50°C. Each pulse shown is the average of 10 pulses at the same temperature and the amplitude of pulses at different temperatures has been normalized to the maximum of the pulse at 20°C. Moreover, the pulse shape for neutron and gamma changes differently with temperature. Shown in Fig. 7 are neutron and gamma pulses detected by NaIL 50°C. Comparing with Fig. 4, it can be seen that the difference in pulse shape between neutrons and gammas is smaller at 50°C than at 20°C. Consequently, the FOM for neutron-gamma discrimination is smaller at 50°C.

Figure 8 displays the FOM for neutron-gamma discrimination versus temperature for the scintillators studied in this work. For CLYC, the FOM for neutron-gamma discrimination continues to improve at low temperatures. Similar results were obtained for a 1 cm<sup>3</sup> CLYC with a 6x6 mm<sup>2</sup> SiPM [6]. This behavior is not observed for CLLB and NaIL. The higher dark current in the SiPMs at higher temperatures contributes to the worsening of the discrimination of neutrons and gammas by PSD. It is interesting to note that while the energy resolution

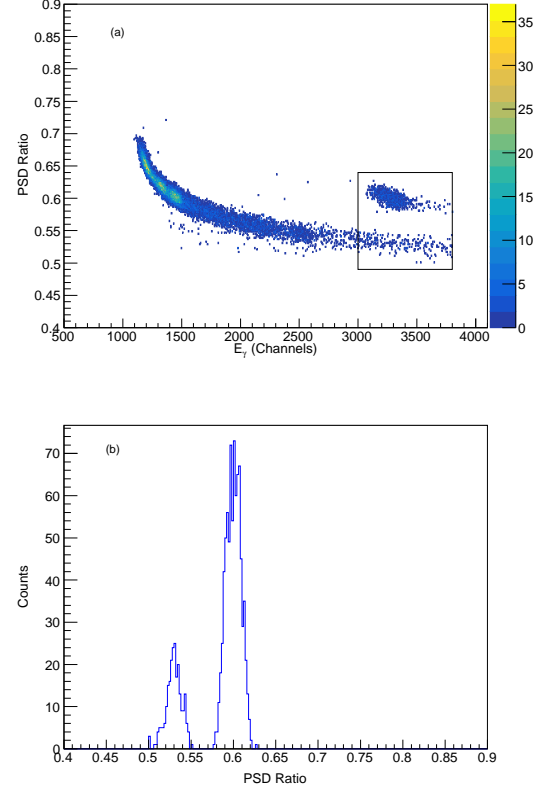


Fig. 5. (a) Scatter plot of PSD ratio versus gamma energy for the measurement with NaIL at 20°. (b) Projection of events in the rectangular area in Fig. 5(a) onto the PSD ratio axis.

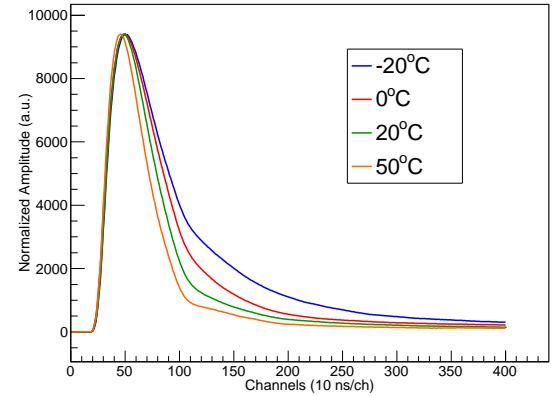


Fig. 6. Pulses for neutrons detected by NaIL for temperatures at -20 (blue curve), 0 (red curve), 20 (green curve), and 50°C (orange curve).

for CLYC\_14 is poor for gamma spectroscopy measurement, this scintillator works well for neutron-gamma discrimination. The newer CLYC sample (CLYC\_16) shows the same FOM for neutron-gamma discrimination as CLYC\_14.

The FOM for neutron-gamma discrimination for NaIL is greater than 2 for all the temperatures. The NaIL scintillator also has the least variation of the FOM with temperature, as shown in Fig. 8. Overall, the FOM is greater than 1 for all three scintillators in the temperature range studied. Therefore,

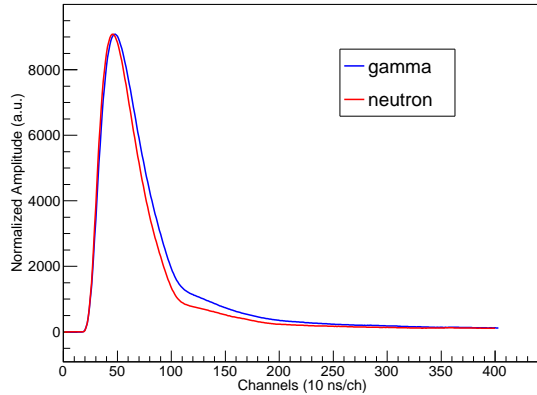


Fig. 7. Pulses for gamma (red curve) and neutron (blue curve) detected by NaIL at 50°C.

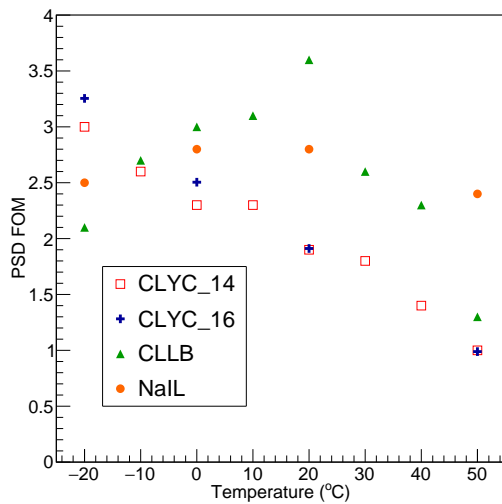


Fig. 8. The FOM for neutron-gamma discrimination as a function of temperature for CLYC\_14 (squares), CLYC\_16 (crosses), CLLB (triangles), and NaIL (circles).

the discrimination between neutron and gamma radiation is acceptable even at high temperatures.

There are actinium contaminants in CLLB which emits alpha-particles. The pulse shape for alphas and neutrons is very similar, as shown in Fig. 3. Moreover, the gamma-equivalent energy for the alpha-particles is greater than 3 MeV. These factors bring challenges in separating neutrons and alphas by PSD, as shown in Fig. 9. Because the CLLB is loaded with natural Li, the efficiency for detecting neutrons from  $^{252}\text{Cf}$  is low. As a result, the neutron peak, located between gamma and alpha peaks in Fig. 9(b), is barely distinguishable from the alpha peak. Although the FOM for neutron-gamma discrimination for CLLB is comparable to that for CLYC and NaIL, the FOM for neutron-alpha discrimination is less than 1 for temperatures between  $-20$  and  $50^\circ\text{C}$ . In spite of the poor neutron-alpha discrimination, the alpha background can be measured,  $3.67 \pm 0.25/\text{min}$ , and corrected for neutron measurements.

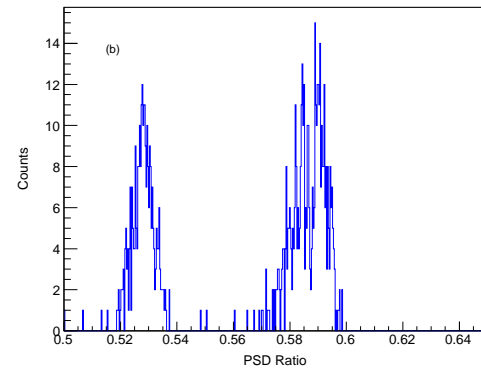
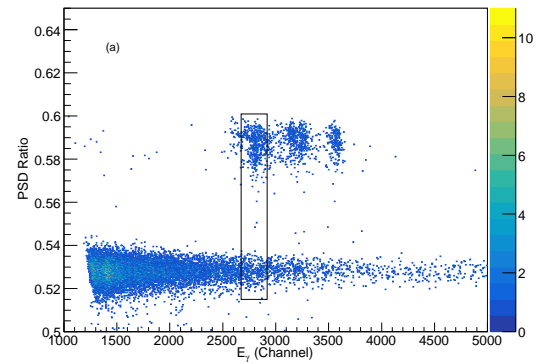


Fig. 9. (a) Scatter plot of PSD ratio versus gamma energy for the measurement with CLLB at  $20^\circ$ . (b) Projection of events in the rectangular area onto the PSD ratio axis.

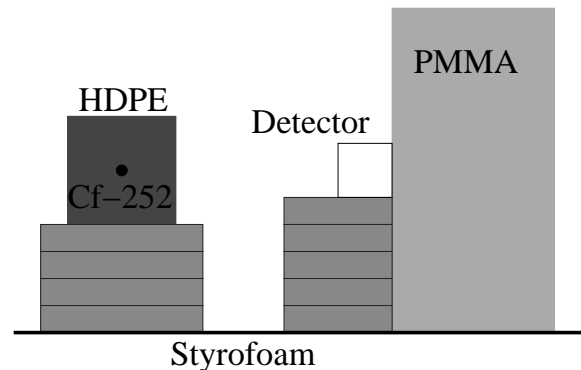


Fig. 10. Apparatus for measuring neutron detection efficiency.

### C. Neutron Detection Efficiency

The efficiency of neutron detection was measured for the three scintillators and compared with a  $\varnothing 15 \times 54 \text{ mm}^3$  8 atm  $^3\text{He}$  tube. As shown in Fig. 10, a  $^{252}\text{Cf}$  source was enclosed in the center of a 10 cm diameter HDPE cylinder and placed 25 cm from the detector. Located behind the detector is a 15 cm thick PMMA block. Both the detector and the neutron source are elevated by Styrofoam pads to reduce the detection of neutrons reflected by the table surface.

The neutron detection efficiency for CLYC, CLLB, and NaIL with respect to the 8-atm  $^3\text{He}$  tube is shown in Table II. The CLYC and NaIL scintillators are loaded with enriched  $^6\text{Li}$

TABLE II  
NEUTRON DETECTION EFFICIENCY FOR CLYC, CLLB (LOADED WITH NATURAL LI), AND NaIL (1.5-INCH CYLINDER) WITH RESPECT TO AN 8-ATM  $^3\text{He}$  TUBE.

scintillator	CLYC	CLLB	NaIL
$\varepsilon/\varepsilon_{He}$	1.9	0.2	1.4

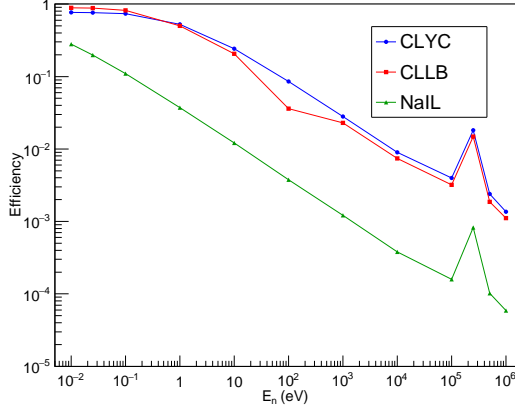


Fig. 11. Results of Geant4 calculations for neutron detection efficiency by 18 mm CLYC, CLLB, and NaIL. The neutron energies are between 0.01 eV and 1 MeV.

whereas the CLLB scintillator is loaded with natural Li. If enriched  $^6\text{Li}$  were used in fabricating the CLLB scintillator, there would be  $2.84 \times 10^{21}$   $^6\text{Li}/\text{cm}^3$  compared to the  $3.46 \times 10^{21}$   $^6\text{Li}/\text{cm}^3$  in CLYC. Therefore, the neutron detection efficiency for CLLB loaded with enriched  $^6\text{Li}$  is expected to be close to CLYC.

Geant4 calculations have been carried out to study the neutron detection efficiency for neutrons incident on an 18 mm of CLLB and CLYC. The neutronHP package was used. A detection event is signified by the generation of a triton-alpha pair in the material. Shown in Fig. 11 are the results of the Geant4 calculations for neutron energies from 0.01 eV to 1 MeV. As discussed above, there is more  $^6\text{Li}$  per volume in CLYC, therefore, the neutron detection efficiency is higher than CLLB. Nevertheless, the neutron capture by  $^{35}\text{Cl}$  at energies below 1 eV competes with that of  $^6\text{Li}$  resulting in the detection efficiency that is lower than CLLB. Additionally, there is a peak at 250 keV which is due to a resonance.

The NaIL scintillator has a larger volume than the CLYC and CLLB used in this work. It is loaded with 0.5 atomic % of  $^6\text{Li}$ . It has been reported that Saint-Gobain will increase the  $^6\text{Li}$  concentration to 1 atomic % for their future NaIL products. On this account, there are  $1.47 \times 10^{20}$   $^6\text{Li}/\text{cm}^3$  in NaIL which is an order of magnitude less than CLYC and CLLB. Because the neutron absorption cross section for both Na and I is substantially smaller than  $^6\text{Li}$ , the neutron detection efficiency for NaIL will not be affected as much as CLYC at low energies. As shown in Fig. 11, the neutron detection efficiency for NaIL is only a factor of 4 less than CLYC at 0.025 eV (thermal energy). However, at higher energies the neutron detection efficiency for NaIL is an order of magnitude lower than CLYC. At these energies, neutron capture by

$^6\text{Li}$  competes more favorably than other elements in CLYC, therefore, the neutron detection efficiency is commensurate with the number density of  $^6\text{Li}$ . Since it is promising to manufacture large size NaIL, this would help increase the neutron detection efficiency [4].

In the future, it would be useful to repeat the measurement of neutron efficiency with enriched  $^6\text{Li}$  loaded CLLB and an 18 mm NaIL cube.

#### IV. CONCLUSION

Three Li-loaded inorganic scintillators, CLYC, CLLB and NaIL, have been tested for neutron and gamma detection for temperatures between  $-20$  and  $50^\circ\text{C}$ . The energy resolution for CLLB is around 4% for the 662 keV gamma-ray which is almost a factor of 2 better than CLYC and NaIL. Pulse-shape discrimination works well in discriminating neutrons from gammas for all three scintillators. In particular, the FOM for neutron-gamma discrimination for NaIL is greater than 2.0 and has the smallest variation with temperatures. The sensitivity for detecting moderated neutrons with CLYC is the highest among these three scintillators and is better than an 8 atm  $^3\text{He}$  tube. The neutron sensitivity is low for CLLB because natural Li is used instead of enriched  $^6\text{Li}$ . According to the experimental results, all three scintillators are suitable for low-power and compact-geometry applications when they are coupled to the custom SiPM array.

#### V. ACKNOWLEDGMENT

We would like to thank S. Lam and S. Swider of CapeSym for preparing and providing the CLYC<sub>16</sub> crystal and A. Zonneveld for loaning the NaIL crystal.

#### REFERENCES

- [1] R.T. Kouzes, A.T. Lintereur, E.R. Siciliano, *Nucl. Instrum. Meth. A*, vol. 784, pp. 172-175, June 2015.
- [2] J. Glodo, W.M. Higgins, D.V.D. van Loef, K.S. Shah, *IEEE Transactions on Nuclear Science*, Vol. 55 (2008) 1206.
- [3] K. Yang, P.R. Menge, J. Lejay, V. Ouspenski, *IEEE Xplore*, DOI: 10.1109/NSSMIC.2013.6829676.
- [4] K. Yang, P.R. Menge, V. Ouspenski, *IEEE Transactions on Nuclear Science*, Vol. 64 (2017) 2406.
- [5] F. Liang, H. Brands, L. Hoy, J. Preston, J. Smith, *IEEE Xplore*, DOI: 10.1109/NSSMIC.2016.8069811.
- [6] K.E. Mesick, L.C. Stonehill, J.T. Morrell, D.D.S. Coupland, *IEEE Xplore*, DOI: 10.1109/NSSMIC.2015.7581936.